J|A|C|S

COMMUNICATIONS

Amyloid β Protein: Aβ40 Inhibits Aβ42 Oligomerization

Megan M. Murray,[†] Summer L. Bernstein,[†] Vy Nyugen,[†] Margaret M. Condron,[‡] David B. Teplow,[‡] and Michael T. Bowers*,[†]

Department of Chemistry and Biochemistry, University of California, Santa Barbara, California 93106-950, and Department of Neurology, David Geffen School of Medicine, and Molecular Biology Institute and Brain Research Institute, University of California, Los Angeles, California 90095

Received December 5, 2008; E-mail: bowers@chem.ucsb.edu

The aggregation of the amyloid β protein (Aβ) is an important event in the development of Alzheimer's disease (AD).[1] Although Aβ40 is ∼10 times more abundant than Aβ42 in vivo, Aβ42 is the primary component of the amyloid deposits that are a hallmark of AD. Studies have also shown that Aβ42 is significantly more neurotoxic than Aβ40.[2] Chemical cross-linking studies have shown that while both Aβ40 and Aβ42 are capable of forming fibrils, they maintain distinct oligomer distributions.[3] For example, Aβ40 and Aβ42 monomers form dimers, trimers, and tetramers in solution. Aβ42, however, may also form pentamers and hexamers, called paranuclei, that self-associate to form dodecamers, protofibrils, and fibrils.[3] In vivo studies in mice and humans suggest that dodecamers of Aβ42 may be the proximate neurotoxins in AD.[4,5]

Recently, new evidence has emerged from in vitro[6,7] and in vivo[8] studies showing that Aβ40, in addition to its unique assembly characteristics relative to Aβ42, may inhibit protofibril and fibril formation by the latter peptide. In this work, we used mass spectrometry coupled with ion mobility spectrometry (IMS)[9−12] to elucidate potential mechanisms for the Aβ40 effect. IMS has successfully been employed in the past to study the structure of Aβ[13,14] and fragments of Aβ.[15,16] For this study, Aβ40 and Aβ42 were synthesized using FMOC chemistry[17] and dissolved separately in a 20 mM ammonium acetate buffer (pH 7.4) at a final concentration of 2 mg/mL. The solutions were combined in a 1:1 Aβ40/Aβ42 ratio and filtered using Macro Spin Column gel filters (The Nest Group, Inc.). The samples were analyzed on a home-built nano-ESI ion mobility mass spectrometer.[18]

The mass spectrum of a 1:1 mixture is given in Figure 1 [spectra and arrival time distributions (ATDs) for other mixtures are given in the Supporting Information (SI)]. Peaks corresponding to the $z/n = -4, -3, -5/2$, and -2 charge states (z = charge, n = oligomer size) are present for both Aβ40 and Aβ42. A third peak is present between the $z/n = -5/2$ peaks for Aβ40 and Aβ42. This peak (m/z 1770) represents the $-5/2$ peak for a mixed oligomer containing equal parts Aβ40 and Aβ42. For a 1:1 mixture, nearly equal intensities are expected for the Aβ40 and Aβ42 monomer peaks ($z/n = -4$ and -3), but clearly the Aβ40 peaks are much larger than the Aβ42 peaks. This result is consistent with the fact that pure Aβ42 oligomerizes much more rapidly than Aβ40, leading to depletion of Aβ42 monomer, and that large aggregates of Aβ42 often clog the nano-ESI spray tip in our experiments. In addition, a 1:2:1 distribution is expected for the $z/n = -5/2$ dimer peaks, but again, the Aβ42-dependent peaks are depleted, supporting the conclusion that rapid Aβ42 aggregation has occurred (see the SI).

IMS makes possible the separation of species that have the same mass-to-charge ratio but differ in shape or size. For IMS separation, the ions pass through a drift cell filled with helium gas (∼5 Torr)
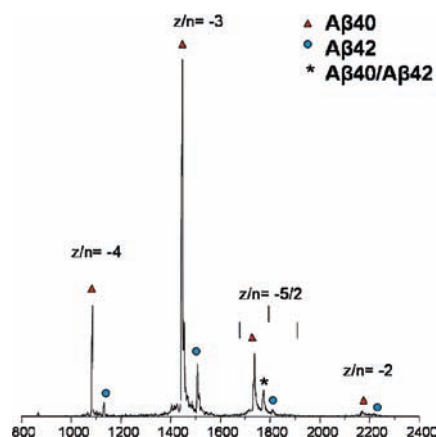
**Figure 1.** Negative-ion mass spectrum of the 1:1 mixture of Aβ40 and Aβ42.

under the influence of a weak electric field, E. This allows species to be separated in time according to their cross sections. If the ions are pulsed into the drift cell, their arrival times at the detector can be measured. Measurements of the ATDs are given in Figure 2 for the three $z/n = -5/2$ peaks in the mass spectrum.

The Aβ40 peak is shown in Figure 2a and is composed of two partially resolved features. The smallest possible oligomer at $z/n = -5/2$ is the $z = -5$ dimer. Injection energy studies (data not shown; see ref 13 for a detailed discussion of injection energy methods) indicate that the feature at longer times (500−525 μs) is strongly favored at high injection energies. Since no new features appear at longer times at the highest injection energies, this peak can be assigned as the $z = -5$ dimer. At the lowest possible injection energies, the shorter time feature (near 430 μs) is favored. Higher-order oligomers with the same value of z/n as lower-order oligomers always appear at shorter arrival times,[13] allowing the 430 μs feature to be assigned as the $z = -10$ tetramer. No other peaks appear in the Aβ40 $z/n = -5/2$ ATD, so under the conditions of our experiment, oligomerization stops at the tetramer.

The ATD for the $z/n = -5/2$ peak of pure Aβ42 is given in Figure 2b. Clearly, this ATD is more complex than that of Aβ40. Again, the various features were assigned previously using injection energy studies.[13] In addition, molecular modeling was performed to assign the qualitative structure of each of the peaks,[19] as noted in the figure. Of interest is the fact that Aβ42 forms a planar cyclic hexamer (a paranucleus), which was previously shown to exist in the Aβ42 oligomer distribution but not in the Aβ40 distribution. This structure is crucial for subsequent oligomerization of Aβ42.[3] Also of interest is the terminal (Aβ42)$_{12}$ species at ∼350 μs, a dodecamer formed by stacking of two planar hexamer rings.[19] The dodecamer has been implicated in memory impairment in transgenic mice[4,20] and in human AD.[5]
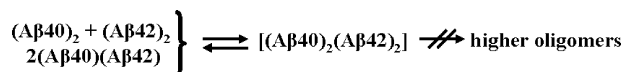
† University of California, Santa Barbara.
‡ University of California, Los Angeles.
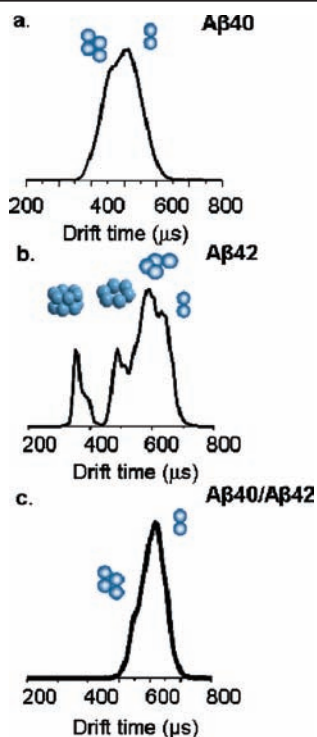
Figure 2. ATDs for the $z/n = -^5/_2$ charge states of (a) Aβ40, (b) Aβ42, and (c) Aβ40/Aβ42.

The ATD for the mixed oligomer (1:1 Aβ40/Aβ42) is given in Figure 2c and shows two incompletely resolved features. Injection energy studies (not shown) indicate that the longer time peak ($\sim$600 μs) is strongly favored at the highest injection energies while the shorter time peak ($\sim$490 μs) becomes more prominent at lower injection energies. These two features are the only ones observed. We assign the $\sim$600 μs peak as the $z = -5$ mixed dimer [(Aβ40)(Aβ42)] and the $\sim$490 μs peak as the $z = -10$ mixed tetramer [(Aβ40)$_2$(Aβ42)$_2$].

Formation of mixed tetramers with 3:1 or 1:3 Aβ40/Aβ42 ratios may be possible, but they are not observed in the mass spectrum (Figure 1). This result supports the formation of the mixed tetramer via dimer condensation rather than sequential monomer addition:

$$\left.\begin{array}{l} (A\beta40)_2 + (A\beta42)_2 \\ 2(A\beta40)(A\beta42) \end{array}\right\} \rightleftharpoons [(A\beta40)_2(A\beta42)_2] \nrightarrow \text{higher oligomers}$$

The second and most important aspect of the mixed oligomer ATD in Figure 2c is that no species larger than tetramers are observed. What this suggests is that Aβ40, which is present at $\sim$10 times the concentration of Aβ42 in a healthy human brain, actually sequesters Aβ42 in stable mixed tetramers, thereby preventing further oligomerization of Aβ42 to form the putative dodecamer toxic agent and consequently potentially deterring the development of AD.

Supporting Information Available: Additional mass spectra of mixtures of different ratios as well as ATDs from the injection energy study of the $z/n = -^5/_2$ peak. This material is available free of charge via the Internet at http://pubs.acs.org.

References

(1) Roychaudhuri, R.; Yang, M.; Hoshi, M. M.; Teplow, D. B. *J. Biol. Chem.* **2009**, *284*, 4749–4753.
(2) Dahlgren, K. N.; Manelli, A. M.; Stine, W. B.; Baker, L. K.; Krafft, G. A.; LaDu, M. J. *J. Biol. Chem.* **2002**, *277*, 32046–32053.
(3) Bitan, G.; Kirkitadze, M. D.; Lomakin, A.; Vollers, S. S.; Benedek, G. B.; Teplow, D. B. *Proc. Natl. Acad. Sci. U.S.A.* **2003**, *100*, 330–335.
(4) Lesne, S.; Koh, M. T.; Kotilinek, L.; Kayed, R.; Glabe, C. G.; Yang, A.; Gallagher, M.; Ashe, K. H. *Nature* **2006**, *440*, 352–357.
(5) Klein, W. L.; Stine, W. B.; Teplow, D. B. *Neurobiol. Aging* **2004**, *25*, 569–580.
(6) Jan, A.; Gokce, O.; Luthi-Carter, R.; Lashuel, H. A. *J. Biol. Chem.* **2008**, *283*, 28176–28180.
(7) Yan, Y. L.; Wang, C. Y. *J. Mol. Biol.* **2007**, *369*, 909–916.
(8) Kim, J.; Onstead, L.; Randle, S.; Price, R.; Smithson, L.; Zwizinski, C.; Dickson, D.; Golde, T.; McGowan, E. *J. Neurosci.* **2007**, *27*, 627–633.
(9) Bowers, M. T.; Kemper, P. R.; Vonhelden, G.; Vankoppen, P. A. M. *Science* **1993**, *260*, 1446–1451.
(10) Clemmer, D. E.; Jarrold, M. F. *J. Mass Spectrom.* **1997**, *32*, 577–592.
(11) Wyttenbach, T.; Bowers, M. T. *Mod. Mass Spectrom.* **2003**, *225*, 207–232.
(12) Vonhelden, G.; Hsu, M. T.; Kemper, P. R.; Bowers, M. T. *J. Chem. Phys.* **1991**, *95*, 3835–3837.
(13) Bernstein, S. L.; Wyttenbach, T.; Baumketner, A.; Shea, J. E.; Bitan, G.; Teplow, D. B.; Bowers, M. T. *J. Am. Chem. Soc.* **2005**, *127*, 2075–2084.
(14) Baumketner, A.; Bernstein, S. L.; Wyttenbach, T.; Bitan, G.; Teplow, D. B.; Bowers, M. T.; Shea, J. E. *Protein Sci.* **2006**, *15*, 420–428.
(15) Murray, M.; Krone, M.; Bernstein, S.; Wyttenbach, T.; Condron, M.; Teplow, D. B.; Shea, J.; Bowers, M. T. Submitted for publication.
(16) Wu, C.; Murray, M.; Bernstein, S.; Condron, M.; Bitan, G.; Shea, J.-E.; Bowers, M. T. *J. Mol. Biol.* **2009**, *387*, 492–501.
(17) Lomakin, A.; Chung, D. S.; Benedek, G. B.; Kirschner, D. A.; Teplow, D. B. *Proc. Natl. Acad. Sci. U.S.A.* **1996**, *93*, 1125–1129.
(18) Wyttenbach, T.; Kemper, P. R.; Bowers, M. T. *Int. J. Mass Spectrom.* **2001**, *212*, 13–23.
(19) Bernstein, S. L.; Dupuis, N. F.; Lazo, N. D.; Wyttenbach, T.; Condron, M.; Bitan, G.; Teplow, D. B.; Shea, J.-E.; Ruotolo, B. T.; Robinson, C. V.; Bowers, M. T. Submitted for publication.
(20) Cheng, I. H.; Scearce-Levie, K.; Legleiter, J.; Palop, J. J.; Gerstein, H.; Bien-Ly, N.; Puolivali, J.; Lesne, S.; Ashe, K. H.; Muchowski, P. J.; Mucke, L. *J. Biol. Chem.* **2007**, *282*, 23818–23828.

JA8092604